FLUCOME 2007
Tallahassee, Florida

ELECTRO-THERMO-HYDRODYNAMIC CONTROL OF SOLIDIFICATION OF BINARY MIXTURES

Marcelo J. Colaço[1] and George S. Dulikravich[2]

ABSTRACT

In this paper we apply a multilevel hybrid optimization algorithm based on a response surface methodology to control the solidification process of a double-diffusive fluid flow, during the phase-change, in the presence of electric and thermal body forces. The problem consists of a rectangular cavity subjected to a thermosolutal flow containing electrically charged particles where the patterns of the isothermal fields for the solute are prescribed. The optimization problem is formulated in terms of the electric and thermal boundary conditions that must induce such prescribed temperature profile. Thus, it is essentially an inverse problem that is solved by determining the appropriate electric and thermal boundary conditions. The electro-thermo-hydrodynamics analysis including solidification was performed using our implicit algorithm on a fixed structured grid. The optimizer is based on several deterministic and evolutionary algorithms with automatic switching among them, combining the best features of each one. The response surface methodology uses several radial basis function interpolants in order to significantly reduce the high computational cost involved during the optimization process of the electric and thermal boundary conditions. The entire numerical simulation was performed on our 96-processor Opteron based parallel computer running Linux and MPI.

Keywords: Electrohydrodynamics, Hybrid Optimization, Response Surface Methods

INTRODUCTION

During solidification from a melt, if the control of melt motion is performed exclusively via an externally applied variable temperature field, it will take quite a long time for the thermal front to propagate throughout the melt thus eventually causing local melt density variations and altering the thermal buoyancy forces. It has been well known that an externally applied steady magnetic or electric field can, practically instantaneously, create additional body forces that influence the flow-field vorticity and change the flow pattern in an electrically conducting fluid (Dulikravich, 1999). Due to the complexity of the combined electro-magneto-hydro-dynamic (EMHD) mathematical model (Dulikravich and Lynn,

[1] Dept. of Mechanical and Materials Engineering, Military Institute of Engineering, Pc. Gen. Tiburcio, 80, Rio de Janeiro, RJ, 22290-270, BRAZIL, Phone: +55 (21) 2546-7264, colaco@ime.eb.br

[2] Dept. of Mechanical and Materials Engineering, Multidisciplinary Analysis, Inverse Design, Robust Optimization and Control – MAIDROC Lab., Florida International University, 10555 West Flagler St., EC 3474, Miami, FL, 33174, USA, Phone: +1 (305) 358-7016, dulikrav@fiu.edu

1997a), the EMHD has traditionally been treated as a separate magneto-hydro-dynamic (MHD) sub-model (Dulikravich and Lynn, 1997b) or a separate electro-hydro-dynamic (EHD) sub-model (Dulikravich and Lynn, 1997b).

A steady state version of EHD solidification analysis without any optimization was studied and published already (Dulikravich et al, 1994). A time-accurate computer code that is capable of simulating EHD flows with phase change for a pure material was also published (Colaço and Dulikravich, 2003). The objective of this work is to combine this analysis code and an optimization code (Colaço and Dulikravich, 2003) in order to minimize the natural convection effects in a cavity filled with a molten material. By minimizing the natural convection effects, it is possible to produce materials with lower thermal stresses than those obtained in the presence of very strong buoyancy forces.

We treated electrodes on the walls of the container as having continuously varying electric field potential. An appropriate variation of the electric potential along the wall electrodes was then determined by using a hybrid optimization algorithm with the objective of minimizing a certain measure (objective function or cost function) quantifying the intensity of local melt flow-field. Simultaneously, the temperature at the boundary of the container was optimized so as to minimize the natural convection effects.

Applicability of this concept is very broad in the general field of manufacturing new functionally graded non-isotropic materials and objects with preferred and vastly different capabilities to deform and conduct electricity and heat in different directions. Since the entire simulation algorithm is time-dependent, the basic concept could be reformulated in the future as an optimal control problem where the intensity variation of the electric field along the boundaries of the solidification container can be also varied in time. This way, desired additives or dopants could be injected and deposited at the desired locations in the advancing solidification front thus creating a truly functionally graded material with a priori specified spatial variation of physical properties and possibly a prescribed variation of microstructure (Rappaz, 1989).

This entire concept is applicable to any molten material that has reasonable electric conductivity, either inherent or because it contains at least a small amount of metal, salts or electrically charged particles.

Two test cases are presented in this proof-of-the-concept paper. The first involves only the optimization of the electric field at the boundaries of the container, while the second involves both the optimization of the electric and the temperature fields. Applying an optimized electric and temperature fields obtained by the use of a hybrid optimizer reduced the natural convection effects.

EHD PROBLEM FORMULATION

The physical problem considered here involves the laminar electrohydrodynamic (EHD) natural convection of an incompressible Newtonian binary mixture. The fluid physical properties are assumed constant. The energy source term resulting from viscous dissipation is neglected and buoyancy effects are approximated by the Oberbeck-Boussinesq hypothesis. Radiative heat transfer, Soret and Dufour effects are neglected.

For the columnar dendritic zone, a porous media model (Voller et al., 1989; Zabaras and Samanta, 2004) must be employed such that the velocity of the solid phase is imposed as zero. Also, the dissipative interfacial stress is usually modeled in an analogy with Darcy law, where the permeability is commonly approximated using the Kozeny-Carman equation (Voller et al., 1989; Zabaras and Samanta, 2004). This

porous media model will not be utilized in this work. In this work, we will use the so-called mushy zone model (Ghosh, 2001; Voller et al., 1989), which is applicable to amorphous materials (waxes and glasses), and the equiaxed zone of metal casting. In this model, the solid is assumed to be fully dispersed within the liquid and the velocity within the solid phase is reduced by imposing a large difference of viscosity between the solid and liquid phases.

The modifications to the Navier-Stokes equations for the EHD fluid flow with heat transfer come from the electro-magnetic force on the fluid where all induced magnetic field terms have been neglected (Dulikravich, 1999; Ko and Dulikravich, 2000; Dulikravich and Lynn, 1997a; 1997b). Then, the Navier-Stokes and the Maxwell equations for the EHD model can be written, for the Cartesian coordinate system as

$$\frac{\partial Q}{\partial t}+\frac{\partial E}{\partial x}+\frac{\partial F}{\partial y}=S \tag{1}$$

$$Q=\lambda\phi \qquad E=(\lambda u+\zeta E_x)\phi^{*}-\Gamma\frac{\partial \phi^{***}}{\partial x} \qquad F=(\lambda v+\zeta E_y)\phi^{**}-\Gamma\frac{\partial \phi^{***}}{\partial y} \tag{2.a-c}$$

where t is the physical time, x and y are the Cartesian coordinates, u and v are the components of the velocity field in the x and y directions and the other quantities, S, λ, ζ, ϕ, ϕ^{*}, ϕ^{**}, ϕ^{***} and Γ, are given in Table 1 for the equations of conservation of mass, species, x-momentum, y-momentum, energy, electric potential and electric charged particles distribution.

Table 1 - Parameters for the Navier-Stokes and Maxwell equations

Conservation of	λ	ζ	ϕ	ϕ^{*}	ϕ^{**}	ϕ^{***}	Γ	S
Mass	ρ	0	1	1	1	1	0	0
Species	ρ	0	C	C	C	C	D	$\nabla\cdot[f_s\rho_s D_s\nabla(C_s-C)]+\nabla\cdot[f_l\rho_l D_l\nabla(C_l-C)]$
x-momentum	ρ	0	u	u	u	u	μ	$-\frac{\partial p}{\partial x}+q_e E_x$
y-momentum	ρ	0	v	v	v	v	μ	$-\frac{\partial p}{\partial y}-\rho g\left[1-\beta(T-T_0)-\beta_S(C-C_0)\right]+q_e E_y$
Energy	ρ	0	h	h	h	T	K	$\sigma\left(E_x^2+E_y^2\right)+q_e\left[uE_x+vE_y+b\left(E_x^2+E_y^2\right)\right]-D_e\left(E_x\frac{\partial q_e}{\partial x}+E_y\frac{\partial q_e}{\partial y}\right)$
Electric potential	0	0	0	0	0	φ	1	$-\frac{q_e}{\varepsilon_0}$
Electric charged particles distribution	1	b	q_e	q_e	q_e	q_e	D_e	0

In Table 1, φ is the electric potential, q_e is the local free electric charge per unit volume, ε_0 is the vacuum dielectric constant or electric permittivity, σ is the electric conductivity, E_x and E_y are the electric field component in x and y-direction, respectively and D_e is the electric diffusion coefficient. C is the concentration of the solute, C_P is the specific heat at constant pressure, D is the mass diffusion coefficient of the solute, g is the acceleration of gravity, h is the enthalpy per unit mass, k is the thermal conductivity, p is the pressure, t is the time, T is the temperature, u and v are the velocity components in the x and y-direction, respectively. x and y are the Cartesian coordinates, β is the thermal expansion coefficient, β_S

is the solute expansion coefficient, μ is the fluid viscosity, ρ is the fluid density, f is the mass fraction. The subscripts 0, l, s, e, m are related to reference value, liquid phase, solid phase, eutectic point and melting point, respectively. The concentration of the solid phase is related to the concentration of the liquid phase, within the mushy region, through the partition coefficient K as $C_s = K\, C_l$.

Note that we used the Oberbeck-Boussinesq approximation for the variation of the density with temperature and concentration in the y-momentum conservation equation. Also note that in the energy conservation equation, the term $C_P T$ was replaced by the enthalpy, h, per unit mass. This is useful for problems dealing with phase change where we could use the enthalpy method (Voller et al., 1989). The above equations were transformed from the physical Cartesian (x, y) coordinates to the computational coordinate system (ξ,η) and solved by the finite volume method. The SIMPLEC method (Van Doormal and Raithby, 1984) was used to solve the velocity-pressure coupling problem. The WUDS interpolation scheme (Raithby and Torrance, 1974) was used to obtain the values of u, v, h, φ and q_e as well as their derivatives at the interfaces of each control volume. The resulting linear system was solved by the GMRES method (Saad and Schultz, 1985).

Details on the derivation of the general model, as well as the concentration transport and energy conservation equations can be found in papers by Colaço and Dulikravich (2005, 2006).

THE RESPONSE SURFACE MODEL

In this paper we used a hybrid optimizer (Colaço and Dulikravich, 2005) based on a highly accurate response surface method (Colaço et al, 2007; Orlande et al, 2007), which uses several radial basis functions - RBF (Hardy, 1971) and polynomials as interpolants. The response surface is capable of interpolating linear as well as highly non-linear functions in multidimensional spaces having up to 500 dimensions (Colaço et al, 2007). Let us suppose that we have a function of L variables x_i, $I = 1,\ldots,L$. The RBF model used in this work has the following form

$$s(\mathbf{x}) = f(\mathbf{x}) = \sum_{j=1}^{N} \alpha_j \phi\left(\left|\mathbf{x}-\mathbf{x}_j\right|\right) + \sum_{k=1}^{M}\sum_{i=1}^{L} \beta_{i,k}\, p_k(x_i) + \beta_0 \tag{3}$$

where $x=\{x_1,\ldots,x_i,\ldots,x_L)$ and $f(x)$ is known for a series of points x . Here, $p_k(x_i)$ is one of the M terms of a given basis of polynomials (Buhmann, 2003). This approximation is solved for the α_j and $\beta_{i,k}$ unknowns from the system of N linear equations, subject

$$\begin{aligned} \sum_{j=1}^{N} \alpha_j\, p_k(x_i) &= 0 \\ &\vdots \\ \sum_{j=1}^{N} \alpha_j\, p_k(x_L) &= 0 \end{aligned} \tag{4}$$

$$\sum_{j=1}^{N} \alpha_j = 0 \tag{5}$$

In this work, the polynomial part of Eq. (3) was taken as

$$p_k(x_i) = x_i^k \tag{6}$$

and the radial basis functions are selected among the following

$$\text{Multiquadrics:} \quad \phi\left(\left|x_i - x_j\right|\right) = \sqrt{\left(x_i - x_j\right)^2 + c_j^2} \tag{7}$$

$$\text{Gaussian:} \quad \phi\left(\left|x_i - x_j\right|\right) = \exp\left[-c_j^2 \left(x_i - x_j\right)^2\right] \tag{8}$$

$$\text{Squared multiquadrics:} \quad \phi\left(\left|x_i - x_j\right|\right) = \left(x_i - x_j\right)^2 + c_j^2 \tag{9}$$

$$\text{Cubical multiquadrics:} \quad \phi\left(\left|x_i - x_j\right|\right) = \left[\sqrt{\left(x_i - x_j\right)^2 + c_j^2}\right]^3 \tag{10}$$

with the shape parameter c_j kept constant as $1/N$. It is used to control the smoothness of the RBF.

From Eq. (3) one can notice that a polynomial of order M is added to the radial basis function. M was limited to an upper value of 6. After inspecting Eqs. (3)-(6), one can easily check that the final linear system has $[(N+M*L)+1]$ equations. Some tests were made using the cross-product polynomials (x_i x_j x_k …), but the improvements on the results were irrelevant. Also, other types of RBFs were used, but no improvement on the interpolation was observed (Colaço et al, 2007; Orlande et al, 2007).

The choice of which polynomial order and which RBF are the best to a specific function, was made based on a cross-validation procedure. Let us suppose that we have *PTR* training points, which are the locations on the multidimensional space where the values of the function are known. Such set of training points is equally subdivided into two subsets of points, named *PTR1* and *PTR2*. The Eqs. (3)-(5) are solved for a polynomial of order zero and for the RBF expression given by Eqs. (7)-(10) using the subset *PTR1*. Then, the value of the interpolated function is checked against the known value of the function for the subset *PTR2* and the error is recorded as

$$RMS_{PTR1,M=0,RBF1} = \sum_{i=1}^{P_{TR2}} \left[s\left(x_i\right) - f\left(x_i\right)\right]^2 \tag{11}$$

Then, the same procedure is made, using the subset *PTR2* to solve Eqs. (3)-(5) and the subset *PTR1* to calculate the error as

$$RMS_{PTR2,M=0,RBF1} = \sum_{i=1}^{P_{TR1}} \left[s\left(x_i\right) - f\left(x_i\right)\right]^2 \tag{12}$$

Finally, the total error for the polynomial of order zero and the RBF expression given by Eqs. (7)-(10) is obtained as

$$RMS_{M=0,RBF1} = \sqrt{RMS_{PTR1,m=0,RBF1} + RMS_{PTR2,m=0,RBF1}} \tag{13}$$

This procedure is repeated for all polynomial orders, up to M=6 and for each one of the RBF expressions given by Eqs. (7)-(10). The best combination is the one that returns the lowest value of the RMS error. Although this cross-validation procedure is quite simple, it worked very well for some standard test cases (Colaço et al, 2007; Orlande et al, 2007).

THE HYBRID OPTIMIZATION ALGORITHM

A hybrid optimization is a combination of the deterministic and the evolutionary/stochastic methods, in the sense that it utilizes the advantages of each of these methods. The hybrid optimization method usually employs an evolutionary/stochastic method to locate a region where the global extreme point is located and then automatically switches to a deterministic method to get to the exact point faster. The base hybrid optimization method, which will be called ***H1*** (Colaço et al, 2004; Colaço et al, 2005), is quite simple conceptually, although its computational implementation is more involved. It uses the concepts of four different methods of optimization, namely: the Broyden-Fletcher-Goldfarb-Shanno (BFGS) quasi-Newton method (Broyden, 1987), the particle swarm method (Kennedy and Eberhart, 1995), the differential evolution method (Storn and Price, 1996) and the simulated annealing method (Corana et al, 1987).

In order to speed-up the optimization task, in real life problems a multilevel approach is utilized, where the optimization procedure is repeated over several levels of grid refinement. Thus, the optimization procedure starts with a very coarse grid and it goes to a finer grid as the iteration continues.

The most frequently utilized module is the particle swarm method, which performs most of the optimization task. The particle swarm method is a non-gradient based optimization method created in 1995 by an electrical engineer (Russel Eberhart) and a social psychologist (James Kennedy) (Kennedy and Eberhart, 1995) as an alternative to the genetic algorithm methods. This method is based on the social behavior of various species and tries to equilibrate the individuality and sociability of the individuals in order to locate the optimum of interest. The original idea of Kennedy and Eberhart came from the observation of birds looking for a nesting place. When the individuality is increased the search for alternative places for nesting is also increased. However, if the individuality becomes too high the individual might never find the best place. In other words, when the sociability is increased, the individual learns more from their neighbor's experience. However, if the sociability becomes too high, all the individuals might converge to the first place found (possibly a local minimum).

In the particle swarm method, the iterative procedure is given by

$$\mathbf{x}_i^{k+1} = \mathbf{x}_i^k + \mathbf{v}_i^{k+1} \tag{14}$$

$$\mathbf{v}_i^{k+1} = \alpha \mathbf{v}_i^k + \beta \mathbf{r}_{1i}\left(\mathbf{p}_i - \mathbf{x}_i^k\right) + \beta \mathbf{r}_{2i}\left(\mathbf{p}_g - \mathbf{x}_i^k\right) \tag{15}$$

where

$\mathbf{x}_i$ is the *i*-th individual of the vector of parameters.
$\mathbf{v}_i = 0$, for $k = 0$.
$\mathbf{r}_{1i}$ and $\mathbf{r}_{2i}$ are random numbers with uniform distribution between 0 and 1.
$\mathbf{p}_i$ is the best value found for the vector $\mathbf{x}_i$.
$\mathbf{p}_g$ is the best value found for the entire population.
$0 < \alpha < 1$; $1 < \beta < 2$

In Eq. (15), the second term on the right hand side represents the individuality and the third term the sociability. The first term on the right-hand side represents the inertia of the particles and, in general, must be decreased as the iterative process proceeds. In this equation, the vector $\mathbf{p}_i$ represents the best value ever found for the i-th component vector of parameters $\mathbf{x}_i$ during the iterative process. Thus, the individuality term involves the comparison between the current value of the i-th individual $\mathbf{x}_i$ and its best value in the

past. The vector $\mathbf{p}_g$ is the best value ever found for the entire population of parameters (not only the i-th individual). Thus the sociability term compares $\mathbf{x}_i$ with the best value of the entire population in the past.

The differential evolution method (Storn and Price, 1996) is an evolutionary method based on Darwin's theory of evolution of the species. This non-gradient based optimization method was also created in 1995 as an alternative to the genetic algorithm methods. Following Darwin's theory, the strongest members of a population will be more capable of surviving under a certain environmental condition. During the mating process, the chromosomes of two individuals of the population are combined in a process called crossover. During this process mutations can occur, which can be good (individual with a better objective function) or bad (individual with a worse objective function). The mutations are used as a way to escape from local minima. However, their excessive usage can lead to a non-convergence of the method.

The method starts with a randomly generated population matrix **P** in the domain of interest. Thus, successive combinations of chromosomes and mutations are performed, creating new generations until an optimum value is found.

In the hybrid optimizer ***H1***, when a certain percent of the particles find a minimum, the algorithm switches automatically to the differential evolution method and the particles are forced to breed. If there is an improvement in the objective function, the algorithm returns to the particle swarm method, meaning that some other region is more prone to having a global minimum. If there is no improvement on the objective function, this can indicate that this region already contains the global value expected and the algorithm automatically switches to the BFGS method in order to find its location more precisely. The algorithm returns to the particle swarm method in order to check if there are no changes in this location and the entire procedure repeats itself. After some maximum number of iterations is performed (e.g., five) the process stops.

THE RESPONSE SURFACE METHOD - HYBRID OPTIMIZER

The new algorithm presented in this paper is an extension of some previously developed algorithms (Colaço and Dulikravich, 2005; Colaço and Dulikravich, 2006), which are based on the evolutionary/stochastic method to locate a region where the global extreme point is located and then automatically switches to a deterministic method to get to the exact point faster. The global procedure is enumerated below:

1. Generate an initial population, using the real function (not the interpolated one) $f(x)$. Call this population P_{real}.
2. Determine the individual that has the minimum value of the objective function, over the entire population P_{real} and call this individual x_{best}.
3. Determine the individual that is more distant from the x_{best}, over the entire population P_{real}. Call this individual x_{far}.
4. Generate a response surface, with the methodology at the previous section, using the entire population P_{real} as training points. Call this function $g(x)$.
5. Optimize the interpolated function $g(x)$ using the hybrid optimizer ***H1***, defined previously, and call the optimum variable of the interpolated function as x_{int}. During the generation of the internal population to be used in the ***H1*** optimizer, consider the upper and lower bounds limits as the minimum and maximum values of the population P_{real} in order to not extrapolate the response surface.
6. If the real objective function $f(x_{int})$ is better than all objective functions of the population P_{real}, replace x_{far} by x_{int}. Else, generate a new individual, using the Sobol pseudo-random (Sobol, 1967)

generator within the upper and lower bounds of the variables, and replace x_{far} by this new individual.

7. If the optimum is achieved, stop the procedure. Else, return to step 2.

From the sequence above, one can notice that the number of times that the real objective function $f(x)$ is called is very small. Also, from step 6, one can see that the space of search is reduced at each iteration. When the response surface $g(x)$ is no longer capable to find a minimum, a new call to the real function $f(x)$ is made to generate a new point to be included in the interpolation. Since the CPU time to calculate the interpolated function is very small, the maximum number of iterations of the ***H1*** optimizer can be very large (e.g., 1000 iterations).

NUMERICAL RESULTS

In this paper we deal with the inverse determination of the electric and thermal boundary conditions that interact with thermal and concentration buoyancies and create such a fluid flow that gives some pre-specified temperature distribution of the solute within a certain region. The geometry considered is a rectangular cavity, whose dimensions are 146 mm x 291 mm. The larger dimension was aligned with the acceleration of the gravity vector. All boundaries were impermeable both to the velocities and to the concentration. The top and bottom walls were kept thermally insulated.

The test cases analysed here involve the fluid flow of Gallium Arsenide (GaAs), whose properties were given in Table 2 (Dulikravich et al., 1994; Sabhapathy and Salcudean, 1990; Brodsky, 1990; Saville and Palusinski, 1986; Eringen and Maugin, 1990).

Table 2 – Physical properties of the media

Property	Value		Property	Value		Property	Value
ρ_l	5320 kg/m^3		b_s	0 m^2/(V.s)		ε_0	8.854 x 10^{-12} kg.m/s^{2}V^2
ρ_s	5320 kg/m^3		D_{el}	0.02 m^2/s		L	726,000 J/kg
C_{Pl}	327 J/kg.K		D_{es}	0 m^2/s		μ_l	2.79 x 10^{-3} kg/m.s
C_{Ps}	327 J/kg.K		β	5.73 x 10^{-6} 1/K		μ_s	2.79 x 10^2 kg/m.s
K_l	46 W/m.K		β_s	0.0875 1/K		D_l	6.04 x 10^{-9} kg/(m.s)
K_s	46 W/m.K		T_0	1511 K		D_s	0 kg/(m.s)
b_l	0 m^2/(V.s)		C_0	0.8 kg/m^3		σ	1x10^{-10} 1/(Ω.m)

The boundaries $x = 0$ and $y = 0$ were submitted to a constant concentration of electric charged particles equal to 1x10^{-6} C/m^2. The initial thermal condition was set to 1511.006 K throughout the fluid in the container, while the melting temperature was set to 1511.005 K and the eutectic temperature was set to 1511 K. The partition coefficient was taken as 0.3. The initial condition for the concentration was set to 0.1 kg/m^3 and the final time of the simulation was 4000 seconds.

The objective function was formulated as a multiobjective function. The objective was to solidify the material as fast as possible (thus, "reducing" the liquid area) and also keep the standard deviation of the vorticity (ω) low within the liquid zone (thus, "reducing" the natural convection effects). Our ultimate objectives are to control local orientations and concentrations of micro particles in the final solid phase. This could be accomplished only if orientations and concentrations of micro particles do not change appreciably in the mushy region while the solidification front passes over such a region. Vorticity causes micro particles in the melt to spin thus causing rapid change in orientation of the micro particles in the

melt. Therefore, one of the objectives was to minimize the vorticity in the melt. The objective function that was minimized was then formulated as

$$F = \left(\text{liquid area fraction}\right)^2 + \sqrt{\frac{1}{\#\text{liquid cells}} \sum_{i=1}^{\#\text{liquid cells}} \left(\frac{\omega_i - \bar{\omega}_i}{\omega_{\max}} \right)^2} \tag{18}$$

where the liquid area fraction varies from 0 to 1 (0 means no liquid area and 1 no solid area). The vorticity was normalized by its maximum value over the entire domain.

The optimization objectives were to be achieved by allowing simultaneous variation of the electric potential at the x and y direction as well as the temperature along the y direction. Two different test cases were analyzed, which are summarized at Table 3. For test case 1, the left and right temperatures are kept fixed, while the electric potentials are optimized both in the x and y directions. It is worth to note that the temperature at the right wall has a linear profile, which was imposed in order to create a stronger natural convection and a more curvilinear solid interface starting at that wall. In the test case 2 the electric potential is also optimized, but the temperature at the right wall is also optimized with a range of temperatures below the melting point. For this test case, the final material should have a greater solid area.

Table 3 – Test cases

Test case	Temperature at x = 0 mm	Temperature at x = 146 mm	Electric potential in x direction	Electric potential in y direction
1	Fixed: 1511.006K	Fixed: 1486.006K-1491.006K (linear profile)	Optimized: 0V-100000V	Optimized: 0V-100000V
2	Fixed: 1511.006K	Optimized: 1391K-1492K	Optimized: 0V-100000V	Optimized: 0V-100000V

The electric potential was discretized at six points equally spaced along the x = 0mm and along y = 0mm boundaries and thermal boundary conditions were discretized at six points equally spaced along the x = 0mm or along x = 146mm boundaries (depending on the test case being analyzed) and interpolated using B-splines for the other points at those boundaries. Thus the number of parameters to be optimized were equal up to 18 (six for the electric boundary conditions at x = 0mm, six for the electric boundary conditions at y=0mm and six for the thermal boundary conditions).

Figure 1 shows the results for the test case 1, where the temperatures at the left and right walls where kept constant and the electric potential along the x and y coordinates were optimized. It can be noticed that the temperature profiles are straight in the vertical direction, showing that the material is solidifying as if it was in the absence of natural convection. Also, it can be noticed that the optimizer tried to achieve the other part of the objective function, which was to maximize the solidified area, as most as possible, since at the final time (4000 s) the temperature profiles start to curve at y = 291 mm. Thus, for a stronger cooling temperature, the vorticity would probably increase, and the temperature profiles would no longer be straight lines, avoiding the first part of the objective function. It can be also noticed that all the void fraction lines have null derivative at the y direction, showing a result close to the one in the absence of natural convection. It is interesting to notice the streamlines within the liquid phase. The electric potential modified the fluid flow in such a way to avoid the curvature of the liquid/solid interface, which is very clear from the visual inspection of the streamlines' patterns (Fig. 1). Figure 2 shows the results for the test case 2, where the electric potential was optimized, as well as the temperature at x = 146 mm. The temperature at this boundary was allowed to vary below the melting point of the material.

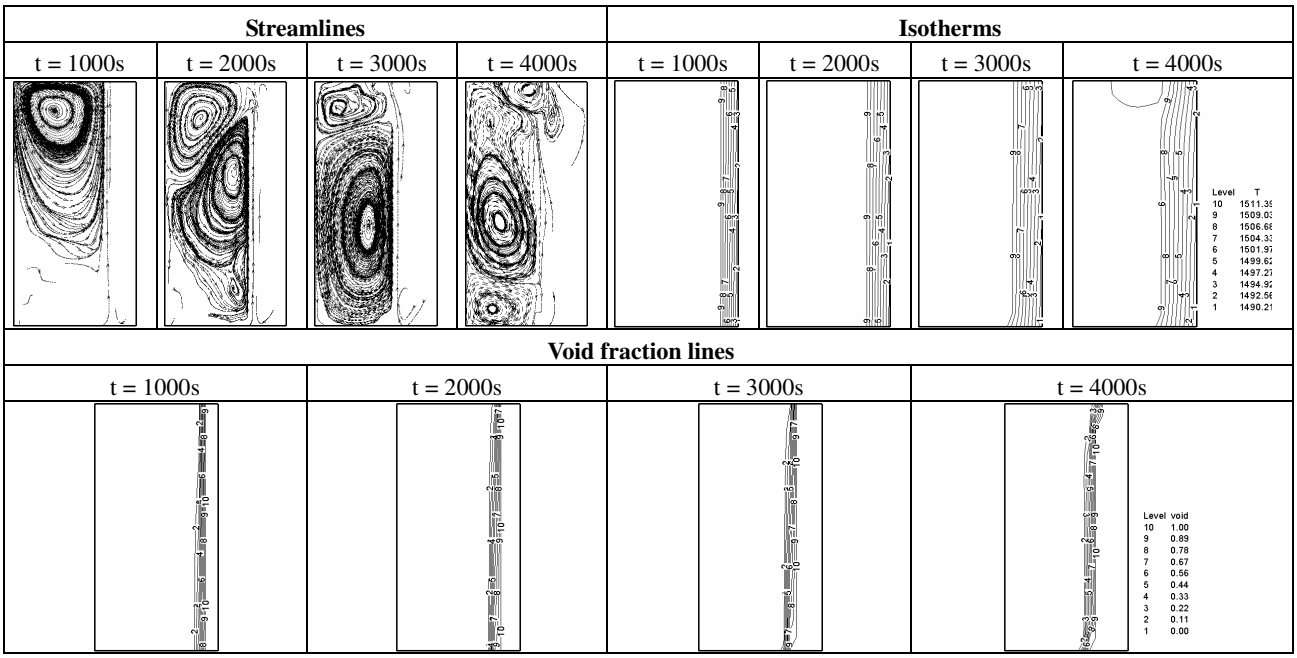

Figure 1 – Results for the test case 1

As one can see from this figure, the solid area is greater then the one obtained in the test case 1. Thus, the optimization of the electric field alone (test case 1) was not capable of minimizing the objective function proposed. The combined use of optimized electric and temperature boundary conditions was more effective in achieving the objective function proposed. Also, the optimizer obtained an electric potential field that tries to keep the isothermals as vertical as possible, in such a way that the solidification front propagates as if it was in the absence of natural convection. The void fraction lines show a profile that tends to be vertical while maximizing the solid area.

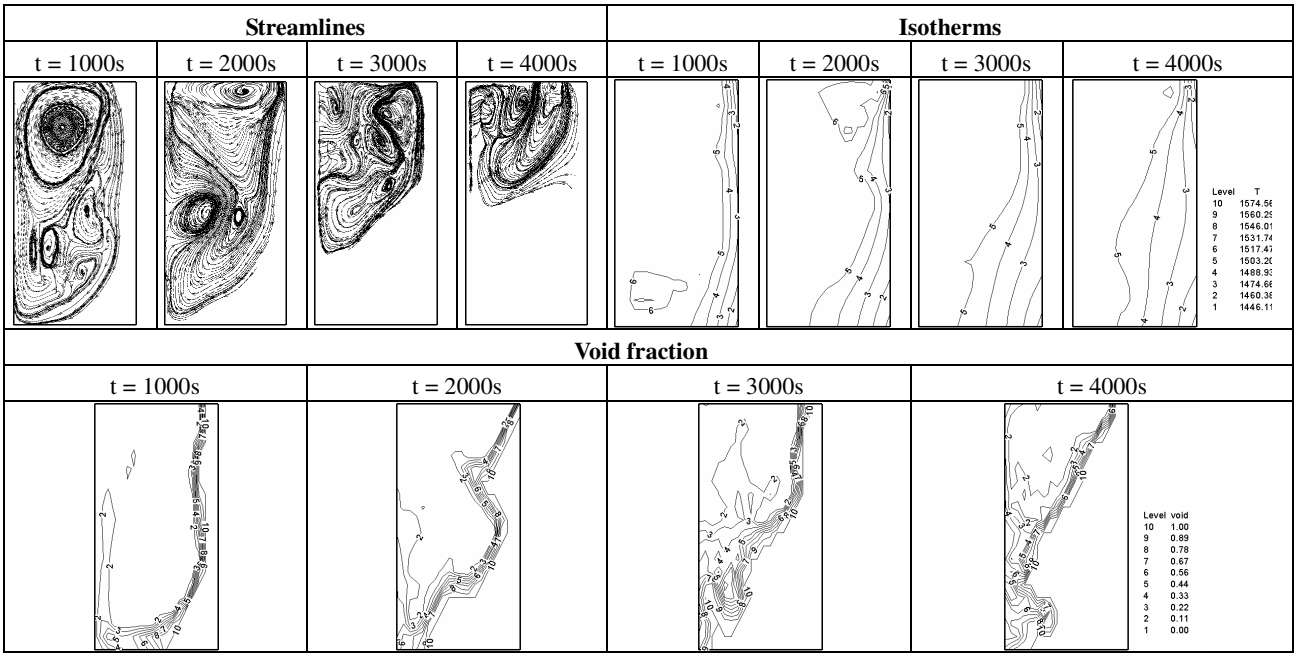

Figure 2 – Results for the test case 2

CONCLUSIONS

In this paper we presented a new hybrid optimizer based on a very accurate response surface model and applied it to an electrohydrodynamic problem, where a binary material was solidifying. The practical problem proposed was formulated as a multiobjective function. The objective was to solidify the material as fast as possible (thus, "reducing"the liquid area) and also keep the standard deviation of the vorticity low within the liquid zone (thus, "reducing" the natural convection effects). A surface response hybrid optimization algorithm was used, which reduced the CPU time required to the minimization of the objective function proposed. The ability to minimize the natural convection effects in problems involving phase change was demonstrated by utilizing an optimized distribution of electric and temperature fields along the boundaries of a solidification container. Transient results were shown where, under the influence of the optimized electric field, both the isothermals and iso-void fraction profiles became more flat. It was shown that the electro-thermo-hydrodynamic optimization is more efficient than the electro--hydrodynamic optimization alone

In this paper the multiobjective formulation as written as a single objective function. However, in future works, a full multiobjective formulation should be explored, creating a Pareto front of all non-dominated solutions.

ACKNOWLEDGMENTS

This work was partially funded by CNPq (a Brazilian council for scientific development). The first author is very grateful to the financial support from FIU (Florida International University).

REFERENCES

Buhmann, M.D., 2003, "Radial Basis Functions on Grids and Beyond", International Workshop on Meshfree Methods, Lisbon.

Brodsky, M. H., 1990, Properties of Gallium Arsenide, 2nd ed., INSPEC, EMIS Datareview Series, no. 2.

Broyden, C. G., 1987, "Quasi-Newton methods and their applications to function minimization", Math. Comp., vol. 21, pp. 368-380.

Colaço, M. J., Dulikravich, G. S. and Martin, T. J., 2003, "Optimization of Wall Electrodes for Electro-Hydrodynamic Control of Natural Convection Effects During Solidification", Materials and Manufacturing Processes, Vol. 19, No. 4, 2004, pp. 719-736.

Colaço, M.J., Orlande, H.R.B. and Dulikravich, G.S., 2004, "Inverse and optimization problems in heat transfer", Invited Lecture, 10th Brazilian Congress of Thermal Sciences and Engineering – ENCIT 2004, Rio de Janeiro, RJ, November 29-December 3, 2004.

Colaço, M.J., Dulikravich, G.S., Orlande, H.R.B. and Martin, T.J., 2005, "Hybrid optimization with automatic switching among optimization algorithms", a chapter in Evolutionary Algorithms and Intelligent Tools in Engineering Optimization (eds: W. Annicchiarico, J. Périaux, M. Cerrolaza and G. Winter), CIMNE, Barcelona, Spain/WITpress, UK, 2005 (ISBN 1-84564-038-1), 2005, pp. 92-118.

Colaço, M. J. and Dulikravich, G. S., 2005, "Obtaining pre-specified concentration profiles in thermosolutal flows by applying magnetic fields having optimized intensity distribution", Int. Conf. on Computational Methods for Coupled Problems in Science and Engineering, COUPLED PROBLEMS 2005, (eds: M. Papadrakakis, E. Oñate and B. Schrefler), Santorini, Greece.

Colaço, M. J. and Dulikravich, G. S., 2006, "A multilevel hybrid optimization of magnetohydrodynamic problems in double-diffusive fluid flow", Journal of Physics and Chemistry of Solids, vol. 67, pp. 1965-1972.

Colaço, M. J., Dulikravich, G. S. and Sahoo, D., 2007, "A comparison of two methods for fitting high dimensional response surfaces", Inverse Problems, Design and Optimization Symposium (IPDO-2007),

(eds: Dulikravich, G. S, Orlande, H. R. B, Colaco, M. J, Tanaka, M.), Miami, FL, April 16-18, 2007.
Corana, A., Marchesi, M., Martini, C. and Ridella, S., 1987, “Minimizing multimodal functions of continuous variables with the ‘Simulated Annealing Algorithm’”, ACM Transactions on Mathematical Software, vol. 13, pp. 262-280.
Dulikravich, G. S., 1999, “Electro-Magneto-Hydrodynamics and Solidification,” Chapter no. 9 in Advances in Flow and Rheology of Non-Newtonian Fluids, Part B (ed. D.A. Siginer, D. De Kee and R.P. Chhabra), Rheology Series, 8, Elsevier Publishers, pp. 677-716.
Dulikravich, G. S. and Lynn, S. R., 1997a, "Unified Electro-Magneto-Fluid Dynamics (EMFD): Introductory Concepts", International Journal of Non-Linear Mechanics, Vol. 32, No. 5, pp. 913-922.
Dulikravich, G. S. and Lynn, S. R., 1997b, "Unified Electro-Magneto-Fluid Dynamics (EMFD): A Survey of Mathematical Models", International Journal of Non-Linear Mechanics, Vol. 32, No. 5, pp. 923-932.
Dulikravich, G. S., Ahuja, V. and Lee, S., 1994, “Modeling of Dielectric Fluid Solidification with Charged Particles in Electric Fields and Reduced Gravity”, Numerical Heat Transfer, Part B, vol. 25, pp. 357-373.
Eringen, A. C. and Maugin, G. A., 1990, Electrodynamics of Continua II – Fluids and Complex Media, Springer-Verlag, New York.
Ghosh, A., 2001, Segregation in cast products, Sadhana, 26, 5-24.
Hardy, R.L., 1971, “Multiquadric Equations of Topography and Other Irregular Surfaces”, Journal of Geophysics Res., Vol. 176, pp. 1905-1915.
Kennedy, J. and Eberhart, R. C., 1995, “Particle swarm optimization”, Proc. of the 1995 IEEE International Conf. on Neural Networks, vol. 4, pp. 1942-1948.
Ko, H.-J. and Dulikravich, G. S., 2000, “A fully non-linear model of electro-magneto-hydrodynamics”, Int. J. of Non-Linear Mechanics, 35 (4) pp. 709-719.
Orlande, H. R. B., Colaço, M. J., Dulikravich, G. S. and Sahoo, D., 2007, “Aproximation of the likelihood function in the Bayesian technique for the solution of inverse problems”, Inverse Problems, Design and Optimization Symposium (IPDO-2007), (eds: Dulikravich, G. S, Orlande, H. R. B, Colaco, M. J, Tanaka, M.), Miami, FL, April 16-18, 2007.
Raithby, G. D. and Torrance, K. E., 1974, “Upstream-Weighted Differencing Schemes and Their Rappaz, M., 1989, “Modelling of Microstructure Formation in Solidification Process”, International Materials Reviews, vol. 34, no. 3, pp. 93-123.
Saad, Y. and Schultz, M., 1985, "Conjugate gradient-like algorithms for solving non-symmetric linear systems," Mathematics of Computation, 44, 170.
Sabhapathy, P. and Salcudean, M. E., 1990, “Numerical Study of Flow and Heat Transfer in LEC Growth of GaAs with an Axial Magnetic Field”, J. Crystal Growth, vol. 104, pp. 371-388.
Saville, D. A. and Palusinski, O. A., 1986, “Theory of Electrophoretic Separation”, AIChE Journal, vol. 32, no. 2, pp.207-214.
Sobol, I. M., 1986, “On the distribution of points in a cube and the approximate evaluation of integrals”, USSR Computational Mathematics and Mathematical Physics, vol. 7, no. 4, pp.86-112.
Storn, R. and Price, K.V., 1996, “Minimizing the real function of the ICEC’96 contest by differential evolution”, Proc. of IEEE Conf. on Evolutionary Comput., pp. 842-844.
Van Doormal, J. P. and Raithby, G. D., 1984, “Enhancements of the SIMPLE Method for Predicting Incompressible Fluid Flow”, Numerical Heat Transfer, vol. 7, pp. 147-163.
Voller, V. R., Brent, A. D. and Prakash, C., 1989, "The Modeling of Heat, Mass and Solute Transport in Solidification Systems", Int. J. Heat Mass Transfer, vol. 32, pp. 1719-1731.
Zabaras, N. and Samanta, D., 2004, “A stabilized volume-averaging finite element method for flow in porous media and binary alloy solidification processes”, Int. J. for Numerical Methods in Eng., 60, pp. 1103-1138.